

# Characterization investigations of glass-ceramics developed from Seyitömer thermal power plant fly ash

M. Erol<sup>a,\*</sup>, U. Demirler<sup>b</sup>, S. Küçükbayrak<sup>a</sup>, A. Ersoy-Meriçboyu<sup>a</sup>, M.L. Öveçoğlu<sup>b</sup>

<sup>a</sup>Department of Chemical Engineering, Chemical and Metallurgical Engineering Faculty, Istanbul Technical University, Maslak 80626, Istanbul, Turkey

<sup>b</sup>Department of Metallurgical and Materials Engineering, Chemical and Metallurgical Engineering Faculty, Istanbul Technical University, Maslak 80626, Istanbul, Turkey

Received 12 February 2002; received in revised form 30 May 2002; accepted 16 June 2002

## Abstract

Glass-ceramic materials were produced from fly ash samples obtained from the Seyitömer thermal power plant in Turkey. Glass samples were crystallized by suitable nucleation and crystal growth heat treatments on the basis of DTA results. The microstructural analysis of glass-ceramic samples were carried out using SEM and XRD techniques. SEM investigations clearly demonstrated the presence of a tiny crystallized phase dispersed in the microstructure. XRD results revealed that the main crystalline phase was diopside [Ca(Mg,Al)(Si,Al)<sub>2</sub>O<sub>6</sub>]. It was observed that the mechanical properties and the thermal expansion coefficient of the glass-ceramic samples depend only on the amount of the crystalline phase. Furthermore, chemical durability of the produced glass-ceramic samples were high.

© 2002 Elsevier Science Ltd. All rights reserved.

**Keywords:** Fly ash; Glass; Glass-ceramic; Mechanical properties

## 1. Introduction

Increasing demands to the generation of more electric power has resulted in construction of coal fired thermal power plants worldwide and thus of the coal consumption and generation of the combustion wastes. Today, thermal power plants exhaust large quantities of combusted waste in the form of bottom ash, fly ash or slag. The growing production of fly ash has long caused an environmental problem with technological and economic effects in the world. Although significant quantities of fly ash are produced permanently in thermal power plants (an annual production of 15 million tonnes in Turkey),<sup>1</sup> only a small amount is utilized, mainly in the concrete, brick or cement production, etc.<sup>2–12</sup> and the remaining is directly discharged into landfills. This is a costly and environmentally unsatisfactory solution. In recent years, many research and

development investigations have been conducted in the utilization of fly ash as a starting material for glass-ceramic production.<sup>13–18</sup> The chemical composition of fly ash is typical of the most common glassy ternary system (SiO<sub>2</sub>–Al<sub>2</sub>O<sub>3</sub>–MgO) with a significant amount of metal oxides which are able to act as nucleant agents for nucleation and crystallization. Furthermore, fly ash is much more convenient than blast furnace and steel slags in glass-ceramic production.<sup>19</sup> It is available in the fine powder form which makes it ready for mixing other ingredients in a batch and in greater quantities than slag.

Glass-ceramics are polycrystalline materials produced by controlled crystallization of suitable glasses during specific heat treatment procedures. The glass-ceramic production process comprises the preparation of a homogeneous glass, the shaping of the glass to produce the required articles and finally the application of a controlled heat treatment process. Controlled heat treatment consists of two steps; nucleation and crystal growth.<sup>20</sup> In the nucleation process, the temperature is held for a sufficient time for stable nuclei formation. Following nucleation, the glass is heated to a higher temperature for a selected period of time, where the

\* Corresponding author. Tel.: +90-212-285-3351; fax: +90-212-285-2925.

E-mail addresses: erolm@itu.edu.tr (M. Erol), ovecoglu@itu.edu.tr (M.L. Öveçoğlu).

crystal growth occurs. The nucleation and crystallization of glasses are important in understanding the stability of glasses in practical applications and in preparing glass-ceramics with desired microstructures and properties.<sup>21</sup>

In the present work, fly ash originating from the Seyitömer thermal power plant was used as a raw material to produce a glass-ceramic material. The main aim of this work is to investigate the effect of different holding times at the crystallization temperature on the microstructure and the properties of the produced glass-ceramic samples and to determine the optimum nucleation and crystallization holding times. For this purpose, microstructural, mechanical, thermal and chemical properties of the glass-ceramic produced from fly ash have been investigated.

## 2. Experimental procedure

### 2.1. Starting materials and glass preparation

Seyitömer thermal power plant fly ash was used in this study as a raw material source. The chemical analysis showed that the fly ash consists of the following oxides (in wt.%): 44.58% SiO<sub>2</sub>, 6.76% CaO, 8.98% MgO, 9.85% Fe<sub>2</sub>O<sub>3</sub>, 22.54% Al<sub>2</sub>O<sub>3</sub>, 0.22% Na<sub>2</sub>O, 0.6% K<sub>2</sub>O. The fly ash used in this study exists in various particle sizes and shapes. As seen in Fig. 1, fly ash particles have various shapes such as spheres, agglomerates and angular shapes. The particle size distribution of the as-received fly ash powders varies between 1–25 µm. X-ray diffraction pattern of the fly ash sample is given in Fig. 2. As seen in Fig. 2, the as-received fly ash comprised the phases: α-quartz (SiO<sub>2</sub>), mullite (Al<sub>6</sub>Si<sub>2</sub>O<sub>13</sub>), enstatite ((Mg, Fe)SiO<sub>3</sub>) and anorthite (CaAl<sub>2</sub>Si<sub>2</sub>O<sub>8</sub>).

Fly ash powders were melted in Pt-crucibles in an electrically heated furnace at 1550 °C for 3 h. No additives or nucleating agents were added to the fly ash batch. To ensure good homogeneity, the melt was poured onto water. After drying and crushing, the melt was remelted at the same temperature level for a time long enough to obtain bubble free melt. This refined melt was

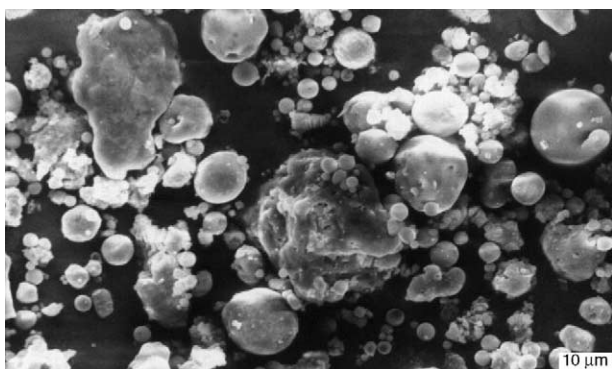


Fig. 1. SEM micrograph of the Seyitömer thermal power plant fly ash.

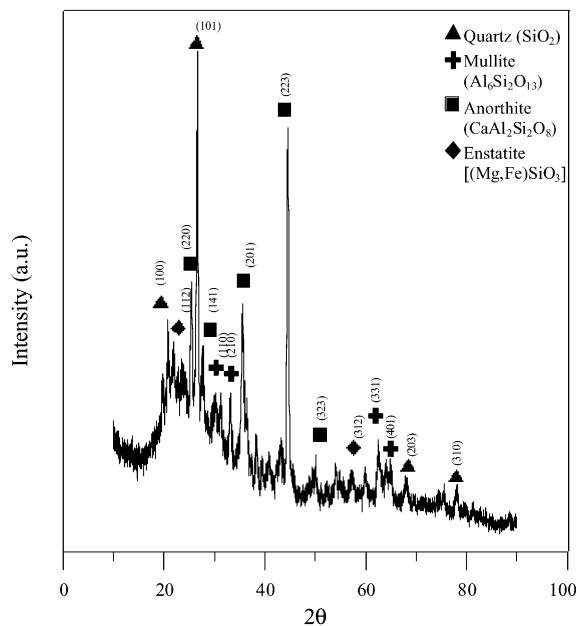


Fig. 2. X-ray diffraction pattern of Seyitömer thermal power plant fly ash.

poured into a preheated graphite mould and a glass having a black colour was obtained. To remove thermal residual stresses, the as-cast glass samples were annealed in a furnace at 600 °C for 2 h followed by slow cooling to room temperature. As reported in detail in a similar study, the annealing temperature and time were chosen as 600 °C and 2 h, respectively.<sup>22</sup> The annealed glass samples were cylindrical in shape having a diameter of 1 cm and length of 1.5 cm.

### 2.2. Thermal analysis and heat treatment

Differential thermal analysis (DTA) scans of the annealed glass samples were carried out in a Rigaku thermoflex thermal analyzer to determine the glass transition temperature ( $T_g$ ), the peak crystallization temperature ( $T_p$ ) and the maximum nucleation time. After crushing annealed glasses to a size of about 1 mm, DTA experiments were performed by heating 30 mg glass samples in a Pt-crucible and using Al<sub>2</sub>O<sub>3</sub> as the reference material in the temperature range between 20 and 1150 °C at a heating rate of 20 °C/min. To achieve complete nucleation, annealed glass samples were heat treated isothermally at the glass transition temperature for 2, 3, 4, 5 and 6 h.

Nucleation and crystallization experiments were carried out on the basis of the DTA scan results. In a previous study,<sup>22</sup> it was determined that 10 °C above the glass transition temperature was sufficient for stable nuclei formation in the microstructure. Since the chemical compositions of fly ashes used in this investigation are similar to the previous study,<sup>22</sup> nucleation and crystallization temperatures were also chosen 10 °C above the  $T_g$  and  $T_p$  values in this study. The annealed glass samples were

heated at a rate of 20 °C/min to the nucleation temperature for the time period required for complete nucleation. Following nucleation, the temperature was raised to the crystallization temperature and held for 15 min, 30 min and 1 h. The crystallized samples were cooled in the furnace. The glass-ceramic samples were shiny dark green.

### 2.3. Microstructural characterization

The microstructural characterization of the produced glass-ceramic samples was carried out using both electron microscopy and X-ray diffraction techniques. Scanning electron microscopy (SEM) investigations were conducted in a Jeol™ Model JSM-T330 operated at 25 kV and linked with an energy dispersive (EDS) attachment. For the SEM investigations, glass-ceramic samples were prepared using standard metallographic techniques followed by chemically etching them in a HF solution (5%) for 1.5 min. The etched glass-ceramic samples were coated with carbon.

The X-ray diffraction (XRD) investigations were performed in a Philips™ Model PW3710 using  $\text{CuK}_\alpha$  radiation at 40 kV and 40 mV settings in the  $2\theta$  range from 10 to 90°. The crystallized phases were identified by comparing the peak positions and intensities with those in the JCPDS (Joint Committee on Powder Diffraction Standards) data files.

### 2.4. Mechanical tests

Vickers microhardness measurements of glass-ceramic samples were carried out using a LL Model Tukon tester. Samples were prepared using standard metallographic techniques and a load of 500 g was used to indent their surfaces. In order to obtain reliable statistical data, at least 15 indentations were made on each sample.

Wear tests were performed on glass-ceramic samples (1×1 cm) using a house-made wear tester. All samples were wear tested under identical conditions of a rotating 60-grit sandpaper used as the hardfacer. A constant perpendicular load of 20 N and a rotational speed of 0.21 m/s was used throughout the tests. Weight loss of the sample was measured and then converted into volume loss using the density. Wear rate values were estimated in volume loss per track length unit. Wear volume and wear rate values were calculated in accordance with the ASTM G 99–90.<sup>23</sup>

### 2.5. Determination of thermal expansion coefficients, density and chemical properties

Thermal expansion coefficient of glass-ceramic samples were carried out using a Netzsch Model DIL 402 PC dilatometer in the temperature range between 100 and 850 °C at the heating rates of 10 °C/min.

Densities of glass-ceramic samples were measured using Archimedes' method in distilled water utilizing buoyancy proportional to the part volume.<sup>24</sup>

Chemical resistance was determined for the amount of weight reduction after being kept for 1 week at 25 °C in a 10%  $\text{HNO}_3$  and for 48 h at 25 °C in a 10% NaOH solutions using polished 1×1.5 cm cylindrical samples. Chemical resistance was also tested in water at 25 °C for 24 h on polished glass-ceramic samples.

## 3. Results and discussion

### 3.1. Thermal analysis and heat treatment

DTA investigations were carried out on annealed glass. DTA thermograms exhibited an endothermic peak corresponding to the glass transition temperature ( $T_g$ ) and an exothermic peak in the temperature range 700–1000 °C denoting the crystallization temperature ( $T_p$ ). Fig. 3 shows the DTA thermogram of the annealed glass sample scanned at the heating rate of 20 °C/min. As seen in Fig. 3, a shallow endothermic peak at 718 °C and a broad exothermic peak at 970 °C correspond to  $T_g$  and crystallization temperature, respectively. As mentioned before, nucleation and crystallization temperatures were chosen 10 °C above the  $T_g$  and  $T_p$  values as 728 and 980 °C, respectively. To determine the maximum nucleation time, annealed glass samples were heated to the glass transition temperature at the heating rate of 20 °C/min and held at this temperature for 2, 3, 4, 5 and 6 h for complete nucleation. The peak crystallization temperature ( $T_p$ ) values were plotted as a function of the nucleation time in Fig. 4. As seen in Fig. 4,  $T_p$  values decrease with the increasing nucleation times. However, for nucleation times longer than 4 h,  $T_p$  values are somewhat close to each other and no further decrease in  $T_p$  values were observed. If the crystallization temperature does not vary with the nucleation time, this case shows that the nucleation stage is fully completed.<sup>21,25</sup> On the basis of this interpretation, a

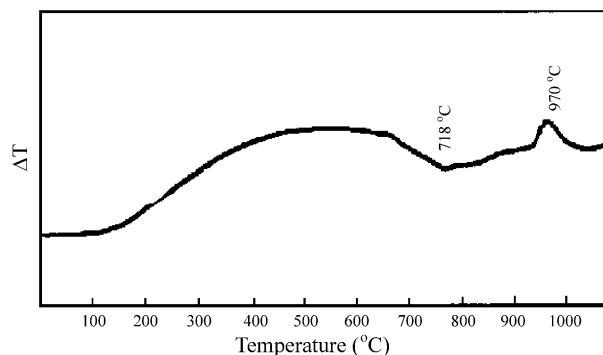


Fig. 3. DTA plot of the glass sample produced from Seyitömer thermal power plant fly ash.

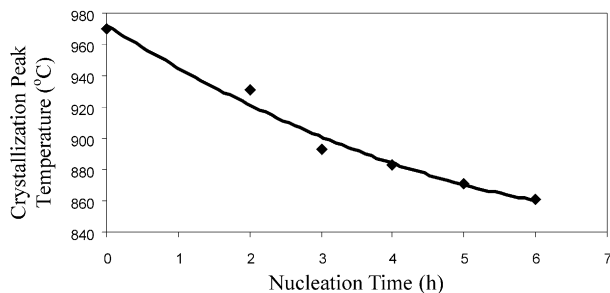


Fig. 4. Crystallization peak temperatures of the glass-ceramic samples plotted as a function of the nucleation time.

nucleation time to achieve optimum conditions was selected as 5 h. According to these DTA results, annealed glass samples were heated at a rate of 20 °C/min to the nucleation temperature and held at this temperature for 5 h. Then, the temperature was raised to the crystallization temperature of 980 °C and the samples were held at this temperature for 15, 30 min and 1 h to examine the effects of the holding time at the crystallization stage on the microstructural, physical and chemical properties of the produced glass-ceramic samples.

### 3.2. Microstructural characterization

X-ray diffractometry (XRD) scans were performed on glass-ceramic samples produced by using different heat treatment schemes. All XRD scans of produced glass-ceramic samples revealed that the main crystalline phase is only diopside-alumina  $[\text{Ca}(\text{Mg}, \text{Al})(\text{Si}, \text{Al})_2\text{O}_6]$ . Fig. 5 shows a representative XRD pattern of the glass-ceramic sample nucleated at 728 °C for 5 h and crystallized at 980 °C for 15 min. As seen in Fig. 5, all the diffraction peaks can be indexed as arising from the reflection planes of the diopside-alumina phase which has a monoclinic structure with lattice parameters<sup>26</sup>  $a = 0.973$  nm,  $b = 0.887$  nm,  $c = 0.528$  nm and  $\beta = 105.92^\circ$ . In a previous study,<sup>27,28</sup> it was found that the main crystalline phase which occurred in the glass-ceramic samples produced from the Çayırhan thermal power plant fly ash was also diopside. As reported in the literature,<sup>20,29–31</sup> the main crystalline phase occurred in the glass-ceramic samples from pure starting materials having similar compositions in the  $\text{SiO}_2\text{–Al}_2\text{O}_3\text{–MgO}$  ternary system was diopside or belonging to the diopside group.

The microstructures of the crystallized glass-ceramic samples were examined by scanning electron microscopy (SEM). Fig. 6 shows the SEM micrograph of the glass-ceramic sample crystallized at 980 °C for 15 min revealing tiny crystallites dispersed in the microstructure. The average crystalline size is about 0.7  $\mu\text{m}$ . Also seen are some glassy regions still remained in the bulk of the sample. Fig. 7 is a SEM micrograph of the

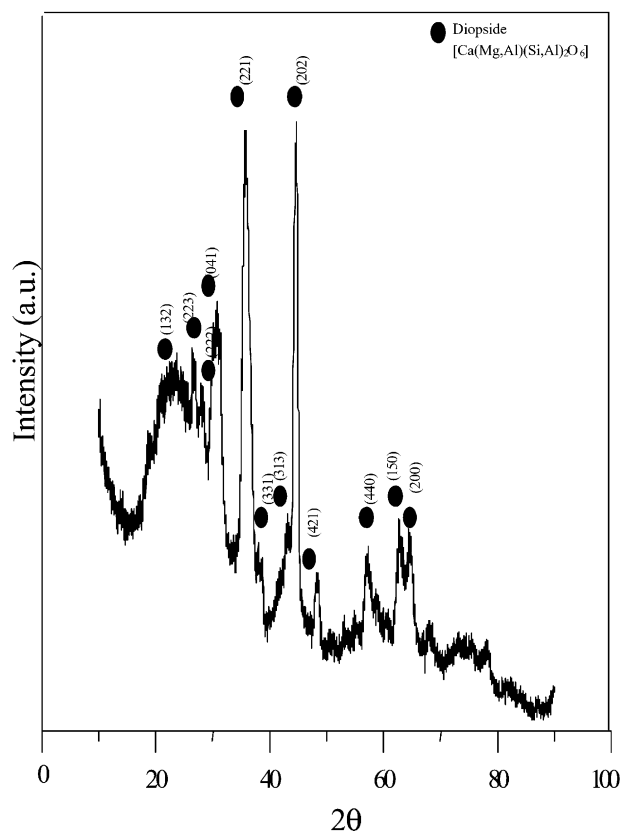


Fig. 5. X-ray diffraction pattern of the glass-ceramic sample nucleated at 728 °C for 5 h and crystallized at 980 °C for 15 min.

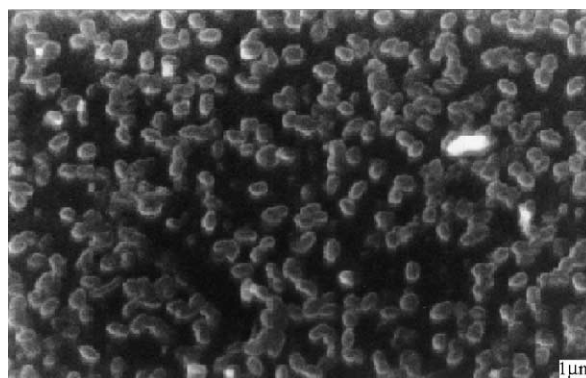


Fig. 6. SEM micrograph of the fly ash-based glass-ceramic nucleated at 728 °C for 5 h and crystallized at 980 °C for 15 min.

glass-ceramic sample crystallized at 980 °C for 30 min. The crystalline size varies between 1 and 1.25  $\mu\text{m}$ . The crystallites are larger than that of the glass-ceramic sample crystallized at 980 °C for 15 min due to longer holding times at the crystallization temperature. It is also seen that the glassy region is smaller than the other sample and the number of crystallites is greater. Fig. 8 is a representative SEM micrograph of the glass-ceramic sample crystallized at 980 °C for 1 h. As seen in Fig. 8, the crystallites have grain size between 1.4 and 1.7  $\mu\text{m}$  and thus are larger than those of the samples crystal-

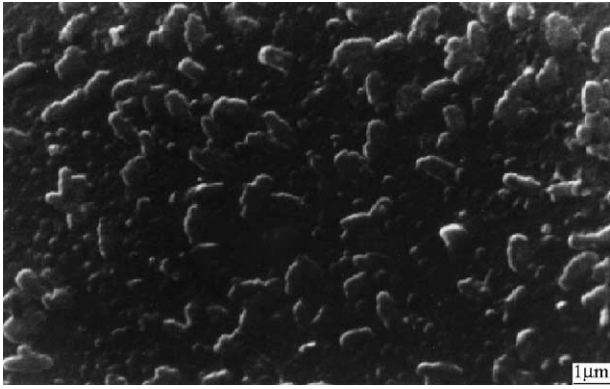


Fig. 7. SEM micrograph of the fly ash-based glass-ceramic nucleated at 728 °C for 5 h and crystallized at 980 °C for 30 min.

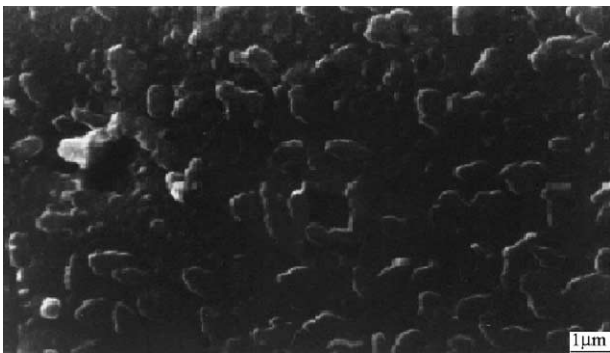


Fig. 8. SEM micrograph of the fly ash-based glass-ceramic nucleated at 728 °C for 5 h and crystallized at 980 °C for 1 h.

lized at 980 °C for 15 and 30 min. The size and the number of crystallites occurred during the heat treatment processes increases. Thus, on the basis of SEM observations, new crystallites developing in the microstructure of the samples and the glassy region decreased with increasing holding times at the crystallization temperature. Furthermore, there are no cracks on the surface of all glass-ceramic samples produced from the Seyitömer thermal power plant fly ash.

### 3.3. Mechanical properties

Fig. 9 shows the error-bar representation of the Vickers microhardness measurements of the glass-ceramic samples. It is clear that the microhardness value increases with the increasing holding times at the crystallization temperature. It can be concluded that with the increase in crystallinity, the hardness values of glass-ceramic samples were also increased. Thus, the glass-ceramic sample crystallized at 980 °C for 1 h has the maximum microhardness value of  $2899 \pm 135$  kg/mm<sup>2</sup>. This value is better than the microhardness values reported by Barbieri et al.<sup>14,17</sup> and Boccacini et al.<sup>30</sup>

Fig. 10 exhibits the wear rate values of the samples crystallized at 980 °C for 15, 30 min and 1 h. As seen in

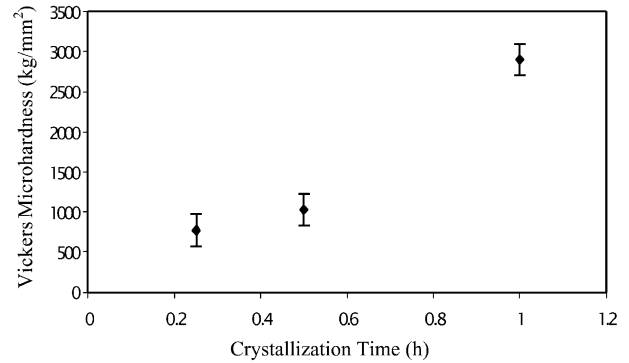


Fig. 9. Vickers microhardness values of the glass-ceramic samples crystallized at 980 °C for 15, 30 min and 1 h plotted as a function of crystallization time.

Fig. 10, wear rate value decreases with the increase in holding time at the crystallization temperature. It can be said that if the number of crystallites increases the resistance to wear decreases. Glass-ceramic sample crystallized at 980 °C for 1 h has the maximum resistance to wear of 3.45 mm<sup>3</sup>/m. This value is better than the value obtained in the previous study.<sup>27,28</sup>

### 3.4. Thermal expansion coefficient, density and chemical properties

Table 1 shows the results of the dilatometry tests, density measurements and chemical durability of glass-ceramic samples. As seen in Table 1, the thermal expansion coefficient of glass-ceramic samples decreased with increasing holding times at the crystallization temperature. It can be concluded that, crystallization greatly improves the heat and thermal shock resistances. Even the minimum thermal expansion coefficient of a glass-ceramic sample crystallized at 980 °C for 1 h is better than the value reported by Romero et al.<sup>32</sup> It is clear that the thermal expansion coefficients of the glass-

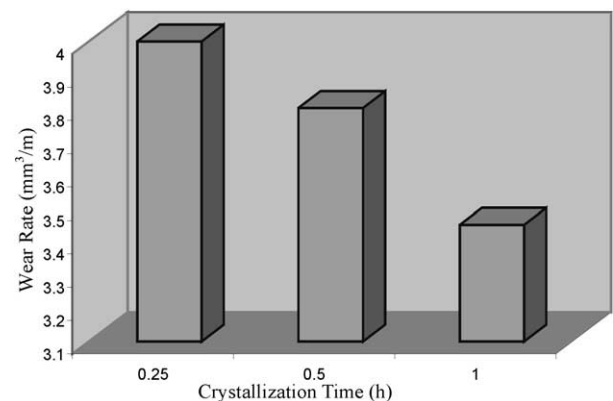


Fig. 10. Wear rate values of the glass-ceramic samples crystallized at 980 °C for 15, 30 min and 1 h plotted as a function of crystallization time.

Table 1  
Some physical and chemical properties of the fly ash based glass-ceramics

Properties	Sample crystallized at 980 °C for 15 min	Sample crystallized at 980 °C for 30 min	Sample crystallized at 980 °C for 1 h
Thermal expansion coefficient (100–850)10 <sup>-7</sup> °C	80.5	76.3	73.1
Density (g/cm <sup>3</sup> )	2.44	3.14	3.29
Water absorption	Negligible	Negligible	Negligible
Weight loss in HNO <sub>3</sub> (g/cm <sup>2</sup> ×10 <sup>-5</sup> )	Negligible	Negligible	Negligible
Weight loss in NaOH (g/cm <sup>2</sup> ×10 <sup>-5</sup> )	Negligible	Negligible	Negligible

ceramics produced from fly ash are higher than commercial glass-ceramics.<sup>33</sup>

Similar to microhardness results, as the glass-ceramic samples become more crystalline, the density of the glass-ceramic samples increases. The density of the glass-ceramic sample crystallized at 980 °C for 1 h is greater than those of the samples crystallized at 980 °C for 15 and 30 min. This result indicates that more than 30 min at the crystallization temperature is needed to ensure the maximum densification. The average density of glass-ceramic samples crystallized at 980 °C for 15, 30 min and 1 h is 2.96 g/cm<sup>3</sup>. This value conforms with the values reported by De Guire et al.<sup>16</sup> for glass-ceramics produced from fly ash and the values given in the literature<sup>20</sup> for glass-ceramics produced from pure starting materials.

Lastly, the water resistance test has shown that no visible etching existed at the surface of the glass-ceramic samples. It was also observed that weight losses in 10% NaOH and in 10% HNO<sub>3</sub> solutions are negligible. It is apparent that the produced glass-ceramic samples show high resistance to acids. This result is better than the values reported by Marghussion et al.<sup>34</sup>

#### 4. Conclusions

This study has clearly shown that glass-ceramic materials can be produced from coal fly ashes. On the basis of the results reported in this study, the following conclusions can be drawn:

1. On the basis of DTA scans, nucleation temperature for fly ash based glass-ceramics was determined as 728 °C with an optimum nucleation time of 5 h.
2. The microstructure of the glass-ceramic samples consists of tiny crystallites varying in size between 0.7 and 1.7 μm. The number and size of the crystallites increase with increasing holding times at the crystallization temperature. X-ray diffraction analysis revealed the presence of only the diopside [Ca(Mg, Al)(Si, Al)<sub>2</sub>O<sub>6</sub>] phase in the produced glass-ceramic samples.
3. Increase in the holding time at the crystallization temperature increases in microhardness values of glass-ceramic samples.
4. Thermal expansion coefficient decreases with the increase of crystallites. The density values and the degree of crystallization increase with increasing the holding time at the crystallization temperature. The glass-ceramic samples show especially high strength and superior acid resistance. Produced glass-ceramic sample with optimum properties for this study is the one crystallized at 980 °C for 1 h.

Overall results have indicated that the glass-ceramic samples produced from coal fly ash have several desirable properties that would make them attractive to industrial use in construction, tiling and cladding applications.

#### References

1. TEAŞ Environmental Presidency, Table of the thermal power plant wastes, 1998.
2. Manz, O. E., Worldwide production of coal ash and utilization in concrete and other products. *Fuel*, 1997, **76**(8), 691–696.
3. Carlsson, C. L. and Adriano, D. C., Environmental impacts of coal combustion residues. *Journal of Environmental Quality*, 1993, **82**(2), 50–55.
4. Anderson, M. and Jackson, G., The beneficiation of power station coal and its use in heavy clay ceramics. *Trans. J. Br. Ceram. Soc.*, 1983, **82**(2), 50–55.
5. Özkan, L., *Effects of Using Fly Ash with Heat Treatments on Concrete Properties*. MS dissertation thesis I.T.U., Istanbul, Turkey.
6. Anderson, M., A new low-cost PFA brickmaking process. In *International Conference on Ash Technology*, 16–22 September 1984, London, pp. 569–573.
7. Helmuth, R., Fly ash in cement and concrete. *Portland Cement Association*, 1987, 203.
8. Yaman, S. and Küçükbayrak, S., Sulfer removal from lignite by oxydesulfurization using fly ash. *Fuel*, 1997, **76**(1), 73–77.
9. Karatepe, N., Meriçboyu, A. E. and Küçükbayrak, S., Preparation of fly ash-Ca(OH)<sub>2</sub> sorbents by pressure hydration for SO<sub>2</sub> removal. *Energy Sources*, 1998, **20**, 945–953.
10. Karatepe, N., Meriçboyu, A. E. and Küçükbayrak, S., Effects of hydration conditions on the physical properties of fly ash-Ca(OH)<sub>2</sub> sorbents. *Energy Sources*, 1998, **20**, 505–511.
11. Karatepe, N., Meriçboyu, A. E., Demirler, U. and Küçükbayrak,

- S., Determination of the reactivity of fly ash-Ca(OH)<sub>2</sub> sorbents for SO<sub>2</sub> removal. *Thermochimica Acta*, 1998, **319**, 171–176.
12. Meriçboyu, A. E., Removal of sulphur dioxide from flue gases. *Energy Sources*, 1999, **21**, 611–619.
  13. Cioffi, R., Pernice, P., Aronne, A. and Quattroni, G., Nucleation and crystal growth in fly ash derived glass. *J. Mater. Sci.*, 1993, **28**, 6591–6594.
  14. Barbieri, L., Manfredini, T., Quralt, I. and Rincan, J. M., Romero, Vitrification of fly ash from thermal power stations. *Glass Technology*, 1997, **38**(5), 165–170.
  15. Dinu, M., Crystallization kinetics of some fly ash glasses. *Materiale de Constructi*, 1986, **28**(2), 131–134.
  16. De Guire, E. J. and Risbud, S. H., Crystallization and properties of glasses prepared from Illinois coal fly ash. *J. Mater. Sci.*, 1994, **19**, 1760–1766.
  17. Barbieri, L., Lancelotti, I., Manfredini, T., Queralt, I., Rincan, J. M. and Romero, M., Design, obtainment and properties of glasses and glass-ceramics from coal fly ash. *Fuel*, 1999, **78**, 271–276.
  18. Cumston, B., Shadman, F. and Risbud, S., Utilization of coal ash minerals for technological ceramics. *J. Mater. Sci.*, 1992, **27**, 1781–1784.
  19. Öveçoğlu, M. L., Microstructural characterization and physical properties of a slag-based glass-ceramic crystallized at 950 and 1100 °C. *J. Eur. Ceram. Soc.*, 1998, **18**, 161–168.
  20. McMillan, P. W., *Glass-ceramics*, 2nd edn. Academic Press, London, New York, San Fransisco, 1979.
  21. Xu, X. J., Ray, C. S. and Day, D. E., Nucleation and crystallization of Na<sub>2</sub>O·2CaO·3SiO<sub>2</sub> glass by DTA. *J. Am. Ceram. Soc.*, 1991, **74**(5), 909–914.
  22. Erol, M., Küçükbayrak, S., Ersoy-Meriçboyu, A. and Öveçoğlu, M. L., Crystallization behavior of glasses produced from fly ash. *J. Eur. Ceram. Soc.*(21), 2835–2841.
  23. ASTM G 99–90, Standard test method for wear testing with a pin-on-disk apparatus.
  24. ASTM C 693–93, Standard test method for density of glass by buoyancy.
  25. Sung, Y. M. and Sung, J. H., Crystallization behavior of calcium aluminate glass fibres. *J. Mater. Sci.*, 1998, **33**, 4733–4737.
  26. *Powder Diffraction File, Card No. 21–1276, Database edn.* Joint Committee on Powder Diffraction Standards (JCPDS), Swathmore, PA, USA, 1992.
  27. Erol, M., Genç, A., Öveçoğlu, M. L., Küçükbayrak, S., Taptık, Y. and Yücelen, E., Characterization of a glass-ceramic produced from thermal power plant fly ashes. *J. Eur. Ceram. Soc.*, 2000, **20**, 2209–2214.
  28. Erol, M., *Utilization of Fly Ash in Glass-ceramic Production*. MS dissertation thesis, I.T.U., Istanbul, Turkey, 1999.
  29. Veasey, T. J., Recent developments in the production of glass-ceramics. *Miner. Sci. Eng.*, 1973, **5**(2), 92–107.
  30. Boccaccini, A. R., Petitmermet, M. and Wintermantel, E., Glass-ceramics from municipal incinerator fly ash. *The American Ceramic Society Bulletin*, 1997, **11**, 75–78.
  31. Alizadeh, P. and Marghussian, V. K., The effect of compositional changes on the crystallization behavior and mechanical properties of diopside wollastonite glass-ceramics in the SiO<sub>2</sub>–CaO–MgO–(Na<sub>2</sub>O) system. *J. Eur. Ceram. Soc.*, 2000, **20**, 765–773.
  32. Romero, M., Rawlings, R. D. and Rincon, J. Ma., Development of a new glass-ceramic by means of controlled vitrification and crystallization of inorganic wastes from urban incineration. *J. Eur. Ceram. Soc.*, 1999, **19**, 2049–2058.
  33. Strnad, Z., *Glass-ceramic Materials*. Elsevier Science, Amsterdam, 1986.
  34. Marghussian, V., Dayi, K. and Niaki, M. H., Effects of composition changes on the crystallization behavior and properties of SiO<sub>2</sub>–Al<sub>2</sub>O<sub>3</sub>–CaO–MgO(Fe<sub>2</sub>O<sub>3</sub>–Na<sub>2</sub>O–K<sub>2</sub>O) glass-ceramics. *J. Eur. Ceram. Soc.*, 1995, **15**, 343–348.